Geophysical Journal International

Advoncing Astronomy and Groupings

Geophys. J. Int. (2022) 228, 1346–1360 Advance Access publication 2021 October 05 GJI Geomagnetism, Rock Magnetism and Palaeomagnetism https://doi.org/10.1093/gji/ggab400

Effect of cyclic loading at elevated temperatures on the magnetic susceptibility of a magnetite-bearing ore

Katarzyna Dudzisz⁶, ^{1,2} Mario Walter, ³ Ralf Krumholz, ³ Boris Reznik¹ and Agnes Kontny¹

¹Institute of Applied Geosciences, Karlsruhe Institute of Technology (KIT), Adenauerring 20a, 76131, Karlsruhe, Germany. E-mail: katarzyna.dudzisz@gmail.com

Accepted 2021 September 30. Received 2021 September 24; in original form 2021 May 30

SUMMARY

Cyclic loading at elevated temperatures occurs either naturally during tectonic or volcanicinduced earthquakes or can be human-induced due to various geological engineering activities. The aim of this study is to test if mechanical fatigue in rocks can be monitored by magnetic methods. For this purpose, the effect of cyclic-mechanical loading (150 \pm 30 MPa) on the magnetic susceptibility and its anisotropy of a magnetite-bearing ore with varying temperatures (400 and 500 °C) and environment (air and vacuum) was investigated. Our study shows that magnetic susceptibility decreases significantly (up to 23 per cent) under air conditions and in vacuum (up to 4 per cent) within the first ca. 1000 cycles. Further loading does not significantly affect the magnetic susceptibility which then remains more or less constant. The decrease of susceptibility parameters is stronger at 500 °C compared to 400 °C under both experimental conditions. Magnetic susceptibility was always measured after decompression of the loaded sample at room temperature so that magnetostriction can be excluded as a reason for these changes. The higher the temperature at which samples were loaded the more pronounced is the oxidation of magnetite to haematite. The transformation of magnetite into haematite under ambient conditions is the most important mechanism influencing bulk magnetic properties. The weak changes in magnetic susceptibility after vacuum loadings are probably caused by intragranular microcracks formed on the surface of magnetite grains. These surface deformation structures are accompanied by the refinement of magnetic domains, which is observed by magnetic force microscopy. Bulk magnetic grain size modifications are also confirmed by hysteresis parameters as well as by the increasing Hopkinson peak ratios determined from magnetic susceptibility measurements over Curie point. The degree of magnetic anisotropy and shape factor only change for the air-treated samples and are therefore related to the haematite formation and not to irreversible ductile deformation in magnetite. Our experimental study shows that cyclic loading can change significantly the magnetic properties of a rock due to mineral transformation below < 1000 cycles and that the first stages of mechanical fatigue, which are a precursor of the failure of rock, are closely associated with these transformations.

Key words: Magnetic properties; Magnetic fabrics and anisotropy; Microstructures.

1 INTRODUCTION

Mechanical stress is known to affect magnetic properties like remanent and induced magnetization and its anisotropy in magnetite (e.g. Nagata & Kinoshita 1964; Stacey 1964; Stacey & Westcott 1965; Nagata 1970; Stacey & Johnston 1972; Martin *et al.* 1978;

Kapička 1988; Johnston 1989). Magnetite is one of the most abundant magnetic minerals in terrestrial rocks, and it is well known that magnetic properties, especially of igneous and metamorphic rocks, respond sensitively to mechanical stresses (Nagata 1970). In the last decade, magnetic parameters have been increasingly used to understand strain behaviour in experimentally deformed rocks (e.g.

²Institute of Geophysics, Polish Academy of Sciences, Warsaw, Ksiecia Janusza 64, PL01452, Poland

³ Institute for Applied Materials, Karlsruhe Institute of Technology, Hermann-von-Helmholtz-Platz 1, 76344, Eggenstein-Leopoldshafen, Germany

Carporzen & Gilder 2010; Till et al. 2012; Volk & Feinberg 2019). Rocks fracture not only under static stresses but also due to repeated loading and unloading, called fatigue loading (Braunagel & Griffith 2019). These dynamic changes are known to enhance rocks' failure at stresses much lower than the yielded stress limit (e.g. Rao & Ramana 1992; Liang et al. 2012). This observation raises the question of whether the magnetic properties of rocks are sensitive to cyclic and fatigue-assisted deformation, especially under seismicrelevant conditions at elevated temperatures near the brittle-ductile transition (Violay et al. 2017). It is well known that large earthquakes induce a dynamic triggering of earthquakes in distant areas (e.g. Johnson & Jia 2005, and references therein). Johnston et al. (2006) also documented magnetic field changes before earthquakes and proved that these changes can be used for monitoring seismic activity. If so, the monitoring of magnetic properties of rocks can provide important information concerning mechanisms of tectonic, volcanic or human-induced seismic deformation.

In the last decade, magnetic parameters have been increasingly used in cyclic loading experiments as a non-destructive method for testing mechanical fatigue in steel. Metal magnetic memory techniques are used to assess stress status, especially for detecting early damage in a ferromagnetic material (Leng *et al.* 2009). Interestingly, cyclically loaded materials can already exhibit changes in microstructures before macroscopic crack initiation begins. Kalkhof *et al.* (2004) describe a linear dependence between low cycle fatigue (< 12 000 cycles) and magnetic susceptibility in austenitic (paramagnetic) steel, which is related to the phase transformation into (ferrimagnetic) martensite.

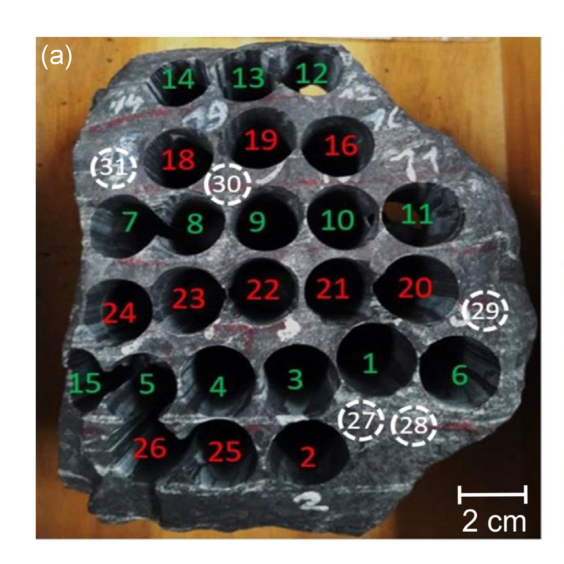
Martin et al. (1978) performed series of cyclic loading experiments up to 200 MPa for titanomagnetite-bearing diabase and argued that changes in induced magnetization are mainly related to differential stress and not to microcrack dilatancy. Anisotropic behaviour of magnetostriction parallel and perpendicular to the uniaxial stress and microstructural changes by strain-induced phase transformations are the most important reasons to explain changes in magnetic susceptibility during static or dynamic compression experiments (e.g. Kalkhof et al. 2004; Gorkunov et al. 2019).

The anisotropy of magnetic susceptibility (AMS) titanomagnetite-bearing basalt and polycrystalline magnetite has been studied under uniaxial static pressures of up to 60 MPa at room temperature by Kapička (1988). He found that with increasing pressure the degree of anisotropy $P(P = K_1/K_3)$, where $K_1 \ge K_2 \ge K_3$ represent the maximum, intermediate and minimum principle susceptibility axis) changes by about 10 per cent and that mean magnetic susceptibility (K_{mean}) decreases parallel and increases perpendicular to the applied stress in agreement with the study of Nagata (1970). Therefore, the magnetic susceptibility of a compressed rock becomes anisotropic. This behaviour is typical for ferrimagnetic minerals with positive magnetostriction when deformed under pressure. Further, Kapička (1988) found that the shape of the AMS ellipsoid of magnetite clearly changes under increasing stress with a decreasing degree of anisotropy and a decrease in the lineation factor (K_1/K_2) . However, after the samples are unloaded, the AMS ellipsoid is reverted nearly completely to its original orientation. These reversible changes are related to the rotation of the spontaneous magnetization within the magnetic domains and their wall displacement. On the other hand, plastic deformation causes irreversible changes of the AMS due to permanent changes of the demagnetization factor. The latter is related to a better arrangement of ferrimagnetic grains or a modification of the shape of these grains and depends on the mechanical properties of the ferrimagnetic minerals and their matrix (Nagata 1970; Owens 1974; Kapička 1988; Hao *et al.* 1997; Till *et al.* 2012; Till & Moskowitz 2013; 2019). Hence, the mentioned results on changes of rock magnetic properties under stress vary due to experimental conditions significantly.

It is well known that dynamic, cyclic loading can reduce rock strength up to 50 per cent due to the accumulation of fatiguedinduced defects (e.g. see Braunagel & Griffith 2019, and references therein). However, there exists a lack of information on the magnetic response to fatigue-induced changes in rocks. Therefore, the aim of this study is to explore the effect of cyclic-mechanical loading on the magnetic susceptibility and its anisotropy of a strongly anisotropic (P ranges from 1.16 to 1.8) metamorphic magnetiterich banded iron ore under various conditions. For this purpose, initial rock samples were comparatively studied with samples deformed in static and dynamic modes. We performed our compression experiments at elevated temperatures (400 and 500 °C) where plastic deformation mechanisms can already occur in magnetite (e.g. Hennig-Michaeli & Siemes 1982), and we compared the compressed samples with those that were only annealed at these temperatures for the same time. The loading conditions of 150 MPa correspond to a depth of approximate 6 km of the upper crust region lying within the seismogenic zone (Lin 2008) with maximum applied pressure below the mechanical strength limit of magnetite which is about 200 MPa (Grosu et al. 2017). In order to better understand the underlying mechanisms of mechanical fatigue, magnetic measurements at room temperatures after loading experiments were combined with non-destructive microstructural observations.

2 MATERIAL AND METHODS

The testing material was banded iron ore from the Sydvaranger mine in Norway, consisting mainly of magnetite (Fe₃O₄) and quartz (SiO₂) and containing amphibole, biotite and pyrite as minor components (further descriptions see Reznik et al. 2016). Fig. 1(a) shows the investigated sample block. Samples marked in red are from magnetite-rich and samples marked in green come from quartz-rich layers. Part of these samples is used for cyclic loading experiments under a normal atmosphere (air). They have a diameter of 1.5 cm and a length of 2.0 cm (sample volume of about 3.3 cm³) or a length of 1.0 cm giving a sample volume of around 1.8 cm³ (Table 1). From the samples with a sample volume of about 3.3 cm³, only the bulk magnetic susceptibility has been measured as the cylinders were too long to satisfy the requirement of an ideal length (l) to diameter (d)ratio of about 0.86-0.9 needed for AMS measurements (Tarling & Hrouda 1993). For samples of 1.0 cm in length, bulk magnetic susceptibility and AMS were measured. Their l/d ratio is 0.67, which is a bit short. However, if magnetic grain sizes are large enough (> 20–40 μ m) and magnetic susceptibility high enough an l/d ratio of 0.66 does not change the AMS values significantly (Ellwood 1979). White dashed circles in Fig. 1(a) show the location of samples used for experiments in a vacuum. These samples have a diameter of 0.7 cm and a length of 0.6 cm (sample volume of about 0.2 cm³), so their l/d ratio is 0.86. For these samples, we also measured bulk magnetic susceptibility and AMS to study the shape parameters of the AMS ellipsoid and if the orientation of the principal magnetic susceptibility axes K_1 , K_2 and K_3 changes. All drilled cores were oriented to the same arbitrary north direction. To inspect the material after each deformation cycle, the top surface of the cylindrical specimen was polished for reflected light microscopy examination. Samples were studied with a Leitz Aristomet or Leitz Orthoplan



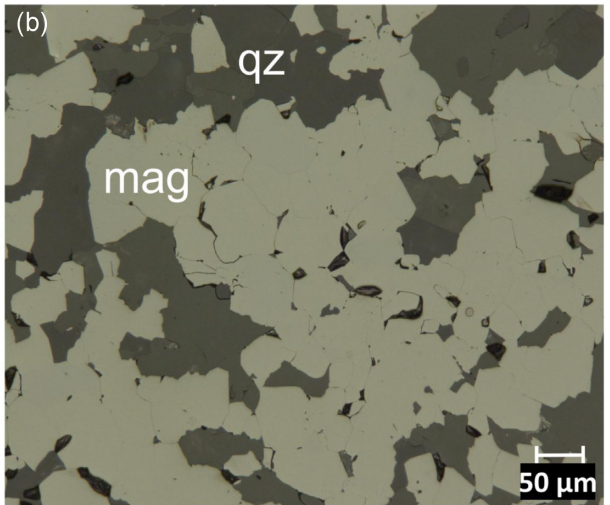


Figure 1. Banded magnetite-quartz iron ore with drillings for compression experiments (a), and microscopic view on a polished surface of an initial sample (b) containing magnetite (mag) and quartz (qz) grains. In (a) red and green numbers correspond to magnetite- and quartz-rich areas, respectively; white dashed circles indicate mini-samples for loadings in a vacuum.

Table 1. Magnetic susceptibility (k_{mean}) of initial samples (Z0 in Table S1, Supporting Information). Bulk is k_{mean} from program SUFAM, AMS- k_i —intrinsic magnetic susceptibility, k_a is apparent susceptibility calculated from AMS mode using eq. (2), P_{in} (T_{in}) and P_{cor} (T_{cor}) are initial and corrected degree of anisotropy (shape parameter), respectively. For areas in hand specimen see Fig. 1(a). Labels e.g. 13_1, 13_2 corresponds to subspecimens of particular sample 13, etc. Samples with a volume of approximate 3.3 and 1.8 cm³ are deformed at a strain rate of 1 kN s⁻¹ (5.66 MPa s⁻¹), vacuum samples (volume of approximate 0.2 cm³) at 115 N s⁻¹ (2.98 MPa s⁻¹).

Sample	Volume (cm ³)	Loading/annealing conditions	Area in hand specimen	Bulk (SI)	$AMS-k_i$ (SI)	k_a (SI)	P_{in}	$P_{\rm cor}$	$T_{ m in}$	$T_{\rm cor}$
Sample	(CIII)		specimen	Duik (51)	$AIVIS^{-}k_l$ (SI)	κ _a (51)	ı ın	1 cor	1 in	1 cor
13_1	3.300	Air, 500 °C, 150 \pm 30 MPa, 1 kN s ⁻¹	Quartz-rich	2.11	_	-	-	-	-	-
13_2	3.290	Air, 500 °C	Quartz-rich	2.33	_	_	-	_	-	_
14_1	3.250	Air, 400 °C	Quartz-rich	2.46	_	_	-	_	-	_
14_2	3.350	Air, 500 °C	Quartz-rich	2.29	_	_	_	_	_	_
15	3.300	Air, 400 °C, 150 \pm 30 MPa, 1 kN s ⁻¹	Quartz-rich	2.74	_	_	_	_	_	_
18_2	3.380	Air, 500 °C, 150 \pm 30 MPa, 1 kN s ⁻¹	Magnetite-rich	3.08	_	_	_	_	_	_
20_2	3.390	Air, 400 °C	Magnetite-rich	2.52	_	_	-	_	-	_
21_1	3.270	Air, 400° C, 150 ± 30 MPa,, $1~\text{kN s}^{-1}$	Magnetite-rich	2.43	_	_	-	_	-	_
21_2	3.190	Air, 500 °C, 150 MPa,	Magnetite-rich	2.27	_	_	_	_	-	_
25_1	1.82	Air, 400 $^{\circ}$ C, 150 \pm 30 MPa	Magnetite-rich	1.69	7.23	2.12	2.827	1.309	-0.501	-0.353
25_2	1.68	Air, 400 °C	Magnetite-rich	1.63	7.78	2.17	2.831	1.281	-0.865	-0.812
25_3	1.86	Air, 500 °C	Magnetite-rich	1.79	8.40	2.21	2.561	1.241	-0.494	-0.353
25_4	1.84	Air, 500 °C, 150 \pm 30 MPa	Magnetite-rich	1.87	9.47	2.28	2.362	1.193	-0.597	-0.483
25_5	1.72	Air, 500° C, 150 ± 30 MPa	Magnetite-rich	1.81	9.84	2.30	2.57	1.206	-0.783	-0.71
27_1	0.17	Vacuum, 400° C, 150 ± 30 MPa	Quartz-rich	1.66	8.44	2.36	3.164	1.384	-0.631	-0.583
27_3	0.12	Vacuum, 500 °C	Quartz-rich	1.34	19.77	2.60	13.687	1.761	-0.134	0.343
28_1	0.22	Vacuum, 500° C, 150 ± 30 MPa	Quartz-rich	1.94	7.61	2.15	2.706	1.365	0.454	0.584
28_2	0.23	Vacuum, 500° C, 150 ± 30 MPa	Quartz-rich	1.67	3.83	1.68	4.554	2.182	0.611	0.723
30_1	0.20	Vacuum, 400 °C	Quartz-rich	1.99	17.96	2.57	2.794	1.157	-0.705	-0.586
30_2	0.19	Vacuum, 400 °C	Quartz-rich	1.70	9.67	2.23	3.402	1.381	-0.541	-0.37
30_7	0.21	Vacuum, 400° C, 150 ± 30 MPa	Quartz-rich	1.83	7.67	2.16	2.863	1.377	0.189	0.36
32_1	0.24	Vacuum, $500 ^{\circ}$ C, 150 ± 30 MPa	Quartz-rich	2.09	12.13	2.41	1.721	1.109	-0.553	-0.474
32_3	0.25	Vacuum, 500° C, 150 ± 30 MPa	Quartz-rich	2.13	11.65	2.39	2.136	1.171	-0.383	-0.25
32_5	0.23	Vacuum, 500° C, 150 ± 30 MPa	Quartz-rich	2.31	21.87	2.64	_	_	_	_

microscope in reflected light mode. From sample 25_5, we prepared a polished section along the long axis of the cylindrical specimen after the cyclic loading experiments. Fig. 1(b) shows a reflected light image of the initial sample with magnetite and quartz where magnetite does not show any oxidation or deformation features. Additionally, the direct imaging of magnetic domains was done under ambient conditions using a commercial magnetic force microscopy (MFM) instrument (Nanoscope IIIs multimode, Bruker AXS) equipped with a PPP-MFMR-10 cantilever (Nanosensors, Switzerland).

2.1 Mechanical test conditions

The experiments were performed in both ambient air and vacuum at elevated temperatures (400 and 500 °C). For air tests, an electromechanical universal testing machine from Instron (type 4505, $F_{\rm max}=50$ kN), equipped with a 5-zone radiation furnace from Prüfer ($T_{\rm max}=1100$ °C) was used. For vacuum tests, however, an electromechanical universal testing machine from Instron (type 8062, $F_{\rm max}=25$ kN), equipped with a high temperature and high vacuum chamber from Maytec ($T_{\rm max}=1600$ °C, p<10–5 mbar)

was used. To simulate a tectonic loading close to reality, the compression tests were conducted load controlled with a stress rate of approximate 5.7 MPa s⁻¹ for samples with a diameter of 1.5 cm and approximate 3 MPa s⁻¹ for samples with a diameter of 0.7 cm by applying a static load $\sigma_{\rm mean}$ of 150 MPa, superimposed by a cyclic load of \pm 30 MPa, resulting in an alternating loading of a sample between $\sigma_{\rm min}=120$ MPa and $\sigma_{\rm max}=180$ MPa. In addition, some tests were performed using a pure static load of 150 MPa.

Furthermore, to evaluate the effect of the test environment on the magnetic properties of the material, the investigations on mechanically tested samples were continuously accompanied by studies on non-loaded but comparable heat-treated specimens. In order to characterize the cycle number after which a significant drop of magnetic susceptibility occurs, we have chosen in our first experimental series in ambient air small step width until 1000 cycles. Then we have chosen one further step at 10 000 in order to see if magnetic susceptibility reaches a 'saturation'. In the second experimental series for the vacuum samples, we have chosen steps over the whole cycling range up to 10 000 because we were interested in the progressive emergence and development of deformation structures. To study these issues the cylinder head planes of the vacuum samples were polished for reflected light inspection.

2.2 Magnetic measurements

Magnetic susceptibility and its anisotropy of all samples were measured using an AGICO Kappabridge KLY-4S after each mechanical/heat treatment step when the sample was cooled to room temperature. The bulk magnetic susceptibility (k) was measured for each sample three times along the cylindrical axis using the software SU-FAM, and a mean value of the three measurements was calculated. AMS was measured with the same instrument using the software SUFAR. The slowly spinning cylindrical samples, adjusted in three perpendicular directions, provided 192 single susceptibility measurements, from which the principal susceptibility axes (K_1, K_2) and K_3) were calculated. Due to a smaller volume of samples (< 3 cm³) than standard (ca. 10 cm³), a special holder for these samples was made of diamagnetic plastic. Because the intrinsic susceptibility of our magnetite samples exceeded the recommended measurement range within AGICO instruments (<0.2 SI) we used a magnetic field of 50 A m⁻¹ (the standard magnetic field is mainly 300 A m⁻¹) for measurements and thus, get lower precision. We observed that the magnetic susceptibility of the same sample measured in the bulk and AMS mode differed significantly due to the demagnetization factor that is included in the AMS measurement mode (Fig. 2). The following equation (e.g. Uyeda et al. 1963) is applied by default in SUFAR mode:

$$k_i = \frac{k_a}{1 - Nk_a} \tag{1}$$

where k_i is intrinsic or 'true' susceptibility, k_a apparent susceptibility and N is a demagnetization factor (N = 1/3 for a sphere; e.g. Stoner 1945; Stacey 1961).

The data presented in Fig. 2 and Table 1 clearly show that the demagnetization factor plays an important role in our high susceptibility specimens with a strong shape anisotropy (which is not the case in 'normal' rocks). To get comparable results of k from bulk and AMS measurements that also consider the shape of the samples, we recalculated the k_a from the k_i values given in the AMS mode using eq. (2) with N = 0.41 and 0.3343 for air- and vacuum-treated samples, respectively. In this paper, k (bulk) will be used to indicate bulk magnetic susceptibility measured using SUFAM mode,

whereas k_a (AMS) will indicate recalculated magnetic susceptibility using SUFAR mode. The degree of anisotropy $(P = K_1/K_3)$ and shape parameter $(T = 2\ln(K_2/K_3)/\ln(K_1/K_3) - 1)$ were computed from recalculated k_a (AMS) of K_1 , K_2 and K_3 , according to Nagata (1961) and Jelinek (1981), respectively (see details in Table 1, Supporting Information).

$$k_a = \frac{k_i}{1 + Nk_i} \tag{2}$$

Temperature-dependent magnetic susceptibility measurements were done for selected samples in the temperature range from -192 to $700\,^{\circ}\mathrm{C}$ to determine possible changes in magnetic mineralogy and transition temperatures after cyclic loading. The high-temperature heating and cooling runs were measured in an argon atmosphere to prevent any oxidation during measurements. An alteration index (Al-index (A₄₀)) was calculated representing the difference between k observed in the cooling and heating curve at $40\,^{\circ}\mathrm{C}$ according to Hrouda *et al.* (2002).

Al-index
$$(A_{40}) = 100 \times (k_C 40 - k_H 40) / k_H 40$$

Hysteresis parameters of selected samples were measured by a Vibrating Sample Magnetometer (VSM, Princeton Measurements) in an applied field of 1 T at the Institute for Rock Magnetism, University of Minnesota, USA.

3 RESULTS

3.1 Magnetic susceptibility of initial samples

Fig. 2 shows the dependence of magnetic susceptibility on the different sample volumes of the initial specimen using the SUFAM and SUFAR mode. It is clear that k_i is significantly higher and shows a stronger variation than k (bulk) which hinders a direct comparison of k from the different measuring modes (see also, Table 1, Supporting Information). The recalculated k_a (AMS) data are similar to the k (bulk) (Table 1 and Figs 2a and b—green circles) although the recalculated values are usually higher by about 8–25 per cent. Samples with the smallest volume are more dispersed due to the lower precision of the measurements in a field of 50 A m⁻¹. Similarly, the degree of anisotropy and shape parameter were affected by the demagnetization factor causing very high P values (Table 1). After recalculation, these values were reduced by 50–55 per cent whereas changes of the T parameter usually did not exceed 30 per cent.

3.2 Magnetic susceptibility parameters in dependence of temperature and confining conditions

3.2.1 Loading experiments in air

Fig. 3 shows the dependence of magnetic susceptibility and anisotropy parameters (degree of anisotropy—*P*, and shape parameter—*T*) with the number of cycling loadings and its time equivalent for samples annealed at 400 and 500 °C in air. The decrease in *k* compared to the initial value reaches for a single specimen up to 23 per cent. The highest drop is always observed during the first 1000 cycles followed by slight changes until 10 000 loadings. However, samples loaded at 500 °C indicate a higher drop than those compressed at 400 °C (Figs 3a and b), which suggests that temperature is the most important factor controlling the magnetic susceptibility decrease. This is confirmed by annealing experiments at 400 and 500 °C (Figs 3a and b), which show a similar

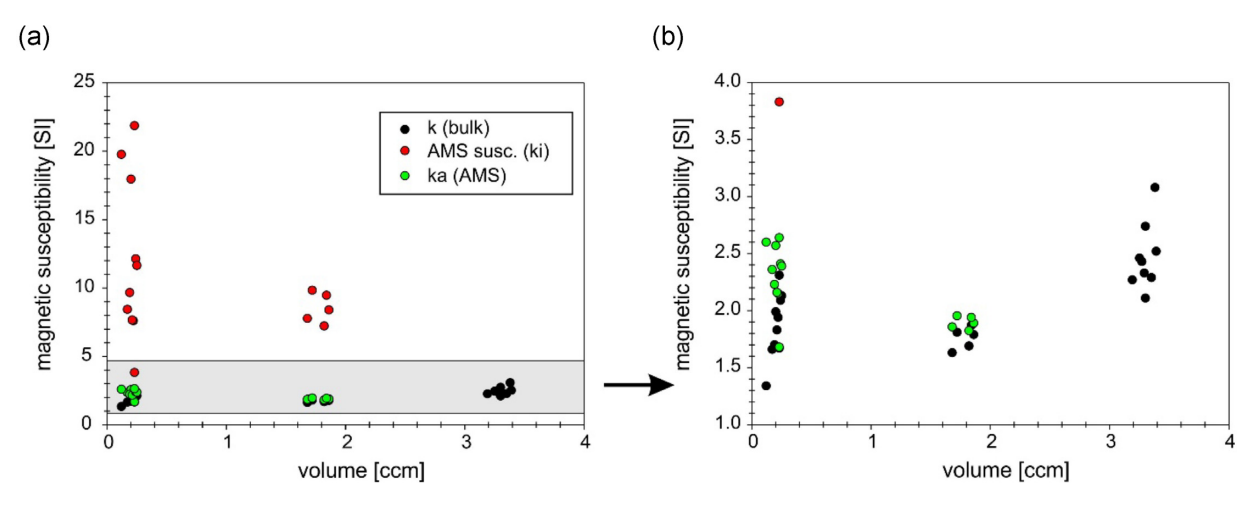


Figure 2. (a) and (b) Comparison of the initial magnetic susceptibility values using different measurement modes. Bulk susceptibility values (k, bulk), AMS susceptibility values (k_i) and recalculated AMS data (k_a, AMS) using eq. (2) are shown by black, red and green symbols, respectively.

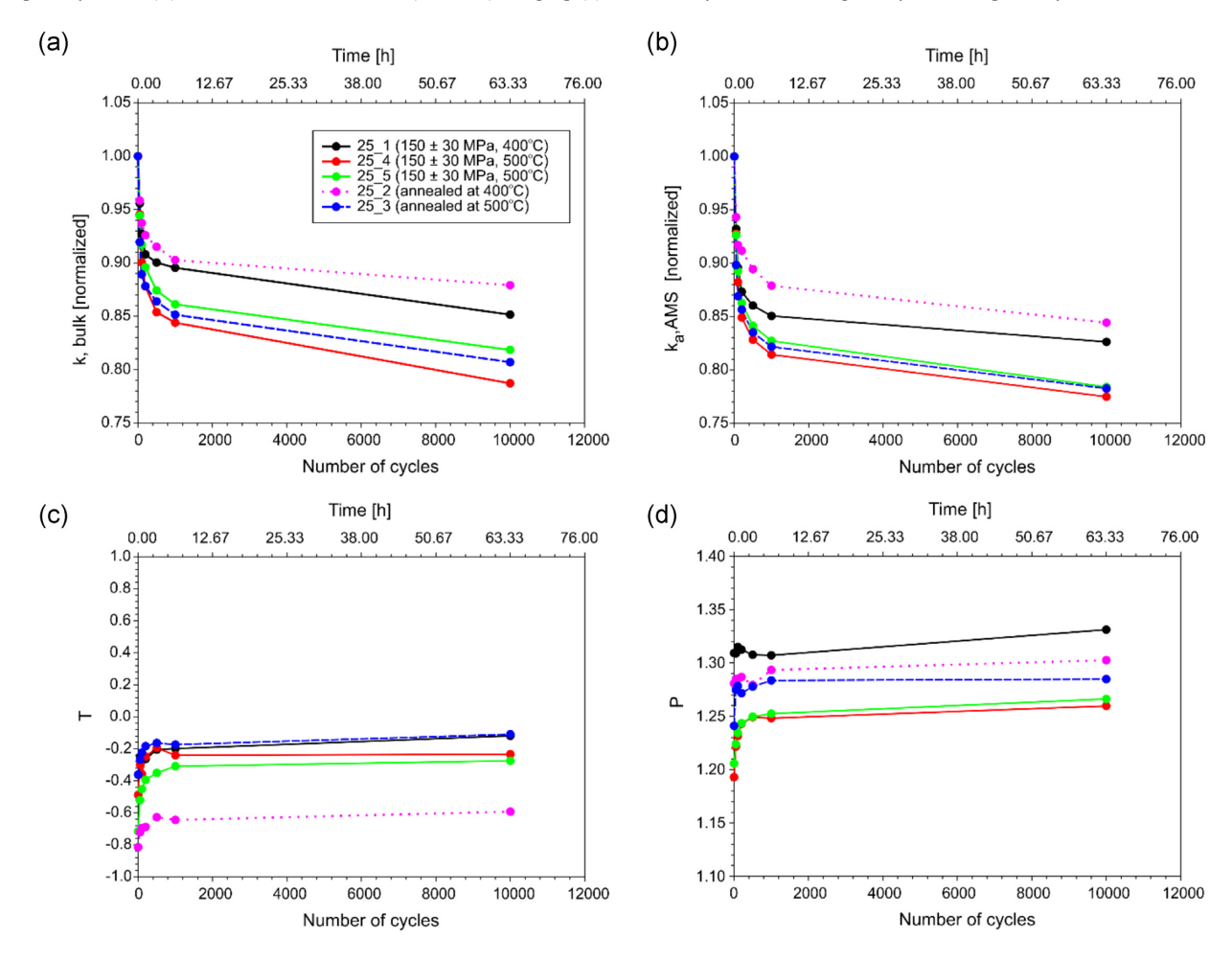
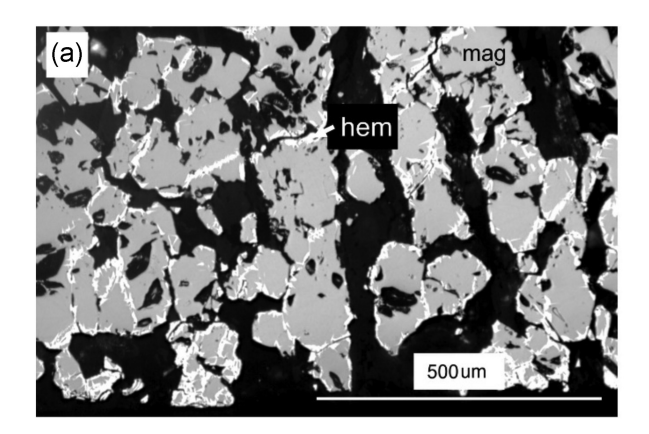


Figure 3. Changes in susceptibility parameters as a function of the number of cycles applied in air loadings. (a) Bulk and (b) recalculated k_a magnetic susceptibility values, changes in the shape parameter T(c), and degree of anisotropy P(d) are shown. For annealed samples at elevated temperatures (dashed lines) annealing time corresponding to cyclic loading time is given on the upper axis.

drop in magnetic susceptibility after about 10 hr heating and a slow further decrease after that time, similar to the cyclic loading experiments. The reason for the drop of the magnetic susceptibility is an oxidation process, which causes the transformation of magnetite ($Fe^{2+}Fe^{3+}{}_2O_4$) to haematite ($Fe^{3+}{}_2O_3$). Fig. 4 shows that the

transformation from magnetite to haematite occurs mainly along grain boundaries and microcracks in magnetite. The oxidation occurs throughout the cylindrical specimen but is more pronounced at the rims. Haematite formation along cracks and fractures seems to be independent of the distance from the rim and is heterogeneously



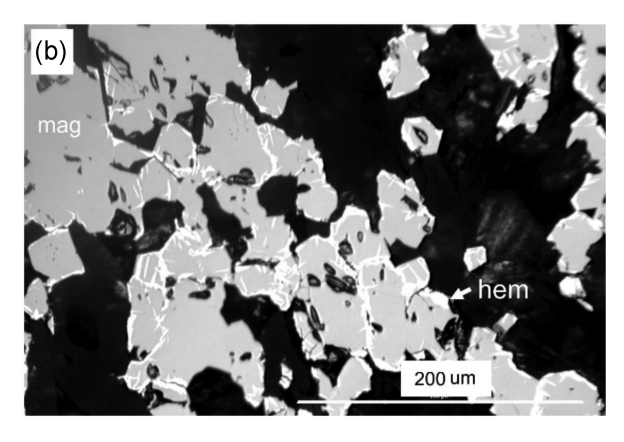


Figure 4. Polished surface parallel to the long axis of the cylindrical sample (parallel to uniaxial compression) of the sample treated in air (25_5) at 10 000 cycles. Magnetite (mag) is grey and haematite (hem) is white (reflected light microscopy, oil immersion). Area (a) is from the rim and (b) from the central part of the polished sample.

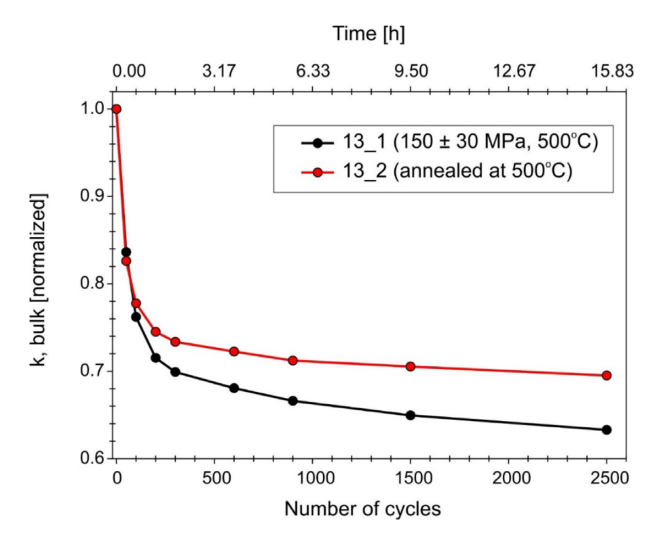


Figure 5. Changes in magnetic susceptibility as a function of the number of cycles for sample 13 (see Fig. 1a). After 100 cycles, the cyclically loaded specimen shows a stronger decrease in magnetic susceptibility than the specimen only annealed in air.

distributed. Fig. 5 shows the cyclic loading experiment and annealing for samples 13_1 and 13_2. With increasing cycling steps, the decrease in magnetic susceptibility is stronger developed than in the only annealed samples at the same time. These observations suggest an effect of deformation on oxidation.

The shape of the AMS ellipsoid also changes with an increasing number of cycling loadings. All samples show a change in the shape parameter (T) from more prolate to triaxial within the first 1000 cycles (Fig. 3c). The degree of anisotropy increases with the number of cycles only in the cyclically loaded samples and those annealed at 500 °C. This process is not very pronounced in samples loaded and annealed at 400 °C (Fig. 3d).

The orientation of principal susceptibility axes during cyclic loading in air atmosphere (initial stage indicated in yellow) does not change significantly and all AMS axes are relatively well grouped during progressive cyclic loading regardless of experimental conditions (Fig. 6). But a small (mostly clockwise in $400\,^{\circ}$ C samples and counterclockwise in $500\,^{\circ}$ C samples) rotation of the horizontally oriented K_1 and K_3 axis is observed in all samples, while the vertically oriented K_2 axis remains relatively stable.

An increase in the number of cyclic loadings causes a decrease in magnetic susceptibility with a slight increment of P at the same time, especially for the 500 °C cyclic loaded samples (Figs 6b, e, h, k and n). In the Jelinek diagram (Jelinek 1981) with T plotted versus P, it is seen that the shape parameter is moving towards a more triaxial shape of the AMS ellipsoid with increasing P (Figs 6c, f, i, l and o). This trend seems to be linear especially for samples subjected to cyclic compression at 500 °C (Figs 6f and i).

3.2.2 Loading experiments in vacuum

In order to study the effect of deformation in the magnetite-quartz ore, we also performed experiments under vacuum and measured the magnetic susceptibility and its anisotropy. These experiments were done with samples of a volume of 0.2 cm³. In contrast to samples loaded in air atmosphere, those subjected to cyclic loading in vacuum show no significant changes in anisotropy parameters P and Twith an increasing number of loading cycles independent of the initial shape of the AMS ellipsoid (Fig. 7). The magnetic susceptibility increases in the first few cycles and then decreases in compressed samples, but this change does not exceed 4 per cent. An exception is seen in the recalculated k_a values of sample 27₋₁ that was loaded at 400 °C where no initial increase in k occurs (Fig. 7b). No significant change in k is seen for samples annealed under vacuum except the sample 30_2 that shows a slight increase in magnetic susceptibility of about 4 per cent (Figs 7a and b; dashed line). As no oxidation is allowed in a vacuum, the changes in the cyclically loaded samples are most likely caused by plastic deformation. Indeed, single hysteresis loops during cycling do not exhibit inelastic strain amplitudes; however, it is observed that the cylindrical samples reveal a continuous decrease in length with an increasing number of cycles with extension perpendicular to compression of 0.3–0.4 per cent. This so-called ratcheting behaviour, characterized by a monotonic increase/decrease of strain at asymmetric cyclic loading, is for example well known for ferritic-martensitic steels (Zhang et al. 2020).

Head planes of the vacuum specimens were polished before the cyclic loading experiments and inspected by reflected light microscopy after a certain number of cycles (Fig. 8). The surface shows slip steps on the magnetite grains. Their number especially increases from 500 to 2000 cycles, but no further significant change occurs between 2000 and 10 000 cycles. As expected, no haematite was observed.

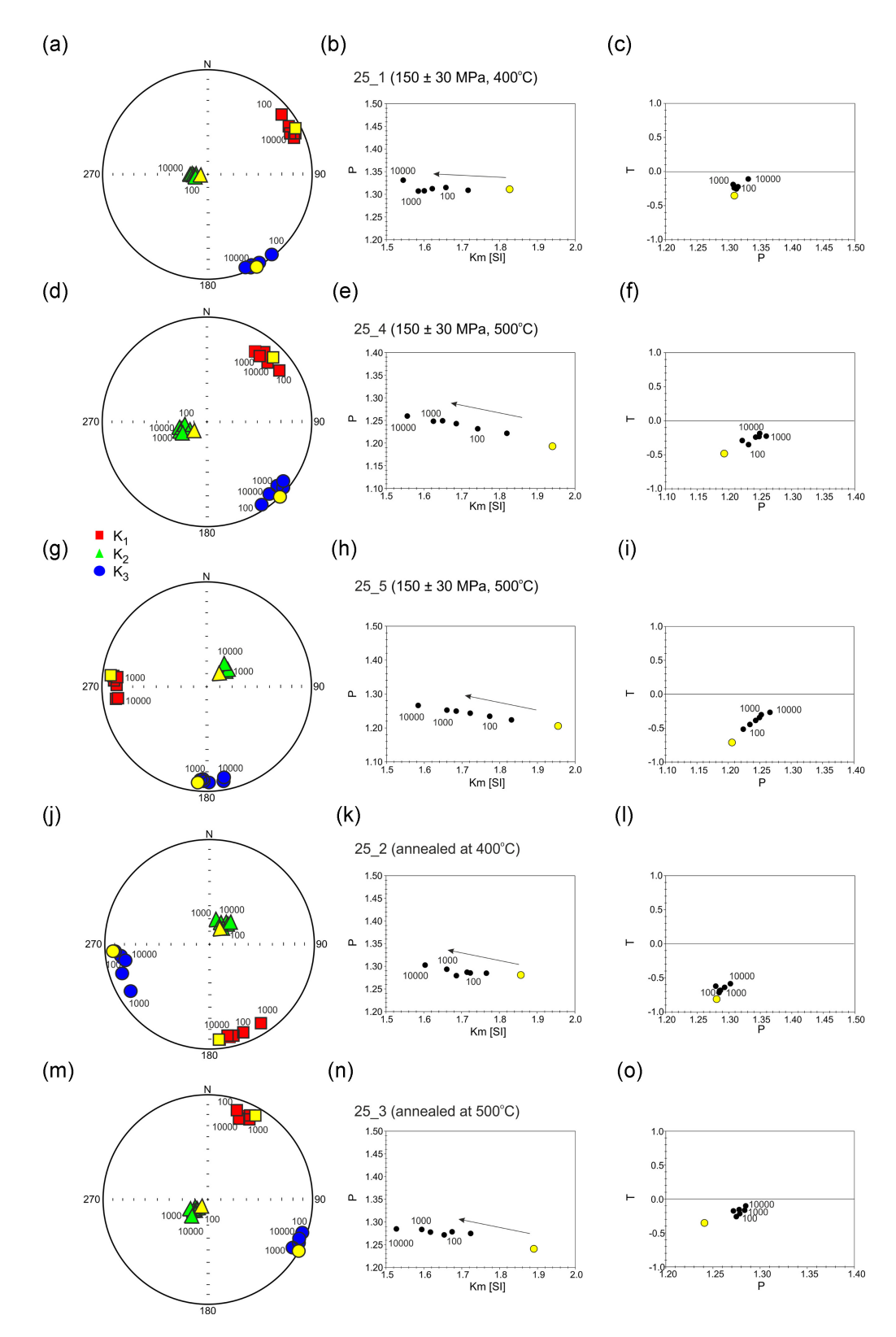


Figure 6. (a), (d), (g), (j) and (m) Orientation of principal susceptibility axes after cyclic loading and (b), (e), (h), (k) and (n) changes in the degree of anisotropy (P) as a function of Km and (c), (f), (i), (l) and (o) shape parameter. K_1 , K_2 and K_3 indicate maximum, intermediate and minimum susceptibility axes. Equal-area lower-hemisphere projections show results in the geographic coordinate system. Values of initial measurement and orientation of susceptibility axes before experiment are indicated in yellow. Experiments in air.

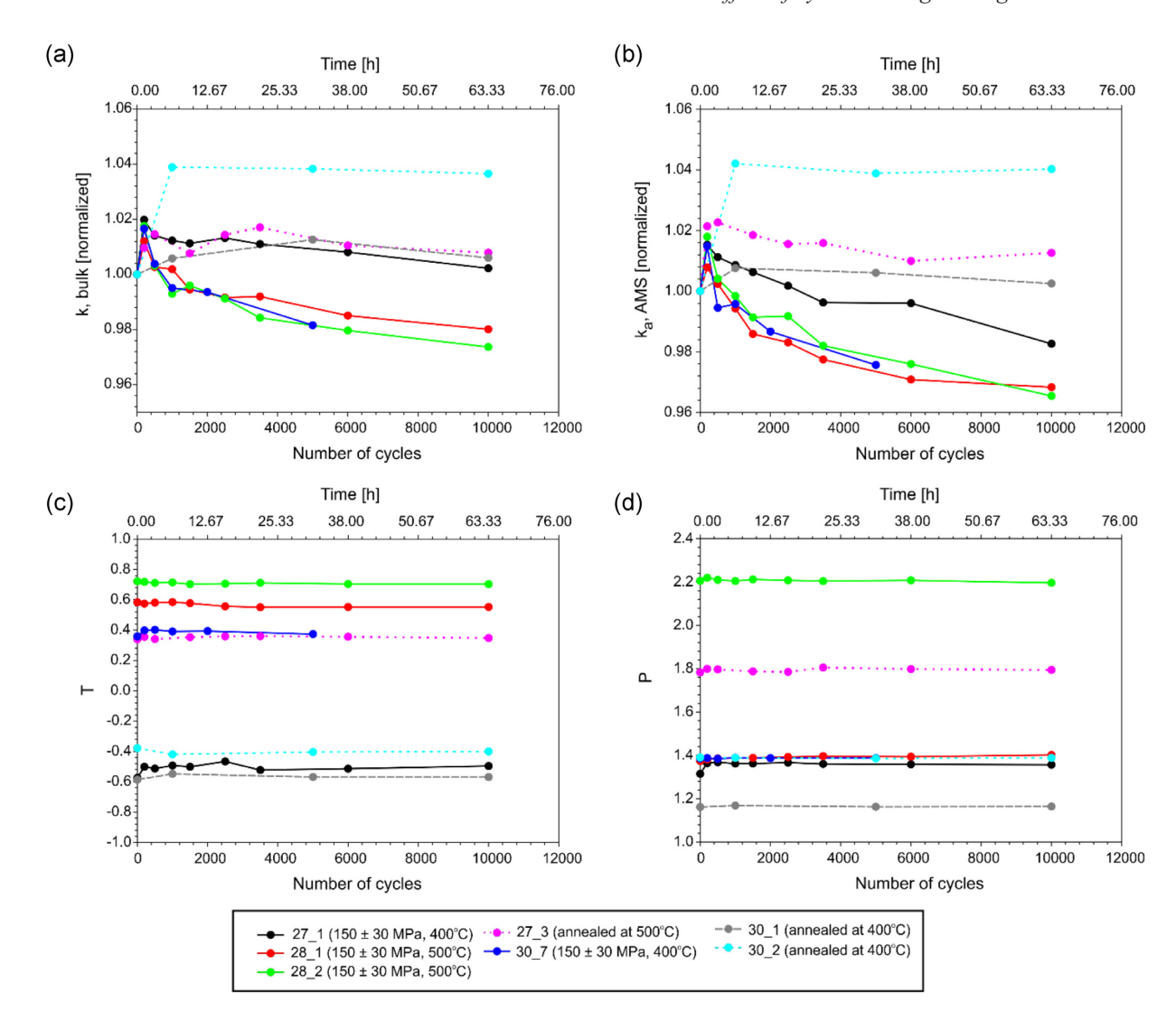


Figure 7. Changes in susceptibility parameters as a function of the number of cycles applied in vacuum loadings. (a) Bulk and (b) recalculated magnetic susceptibility variations, changes in the shape parameter T(c), and degree of anisotropy P(d) are shown. For annealed samples at elevated temperatures (dashed lines) annealing time corresponding to cyclic loading time is given on the upper axis.

Principal AMS axes are quite well grouped regardless of loading conditions (Fig. 9), but again the horizontally oriented principle susceptibility axes of some samples change slightly their orientation, while the vertically oriented sample remains vertical with no variation. Only in samples where the steep principle susceptibility axis is oblique by more than approximate 20° this axis also shows some variation. In the vacuum experiments, the shape parameter T is not changing but there is a weak trend of slightly increasing degrees of anisotropy P in the cyclic loaded as well as in the annealed samples.

3.3 Oxidation and magnetic domain reduction deduced from magnetic measurements

Temperature-dependent magnetic susceptibility measurements (k–T curves) for initial, annealed, static compressed and cyclically compressed magnetite-quartz ore in air and vacuum (Fig. 10) revealed magnetite as the dominant ferrimagnetic mineral showing a Curie temperature (T_C) between 577 and 580 °C and a sharp Verwey transition (T_V) in a range from 118 to 121 K (Table 2). The initial ore shows the lowest T_V and the highest T_C in comparison to

the annealed and deformed samples. High-temperature curves are quasi-reversible for the initial ore and vacuum-treated samples, and become irreversible in all air-treated specimens. Therefore, high-temperature k–T curves were used for calculation of the alteration index (A_{40}), providing information on the degree of alteration during measurements (Table 2).

Very low positive or negative values of A_{40} were calculated for the initial ore and the vacuum-treated sample indicating nearly no oxidation or other heating-induced transformations. This observation is in agreement with the optical investigations (Figs 1b and 8). Samples treated in air show much higher values of A_{40} , and an increase from the only annealed to the static and cyclic loaded samples is observed. We interpret the positive values of the alteration index as a result of the retransformation of haematite into magnetite during the temperature-dependent magnetic susceptibility measurements in an argon atmosphere. The more haematite is produced during treatment (annealing only or heating and deformation; see Fig. 4), the higher is the alteration index.

In the low-temperature *k*–*T* curves, a slightly stronger drop in the magnetic susceptibility compared to the initial sample occurs in the

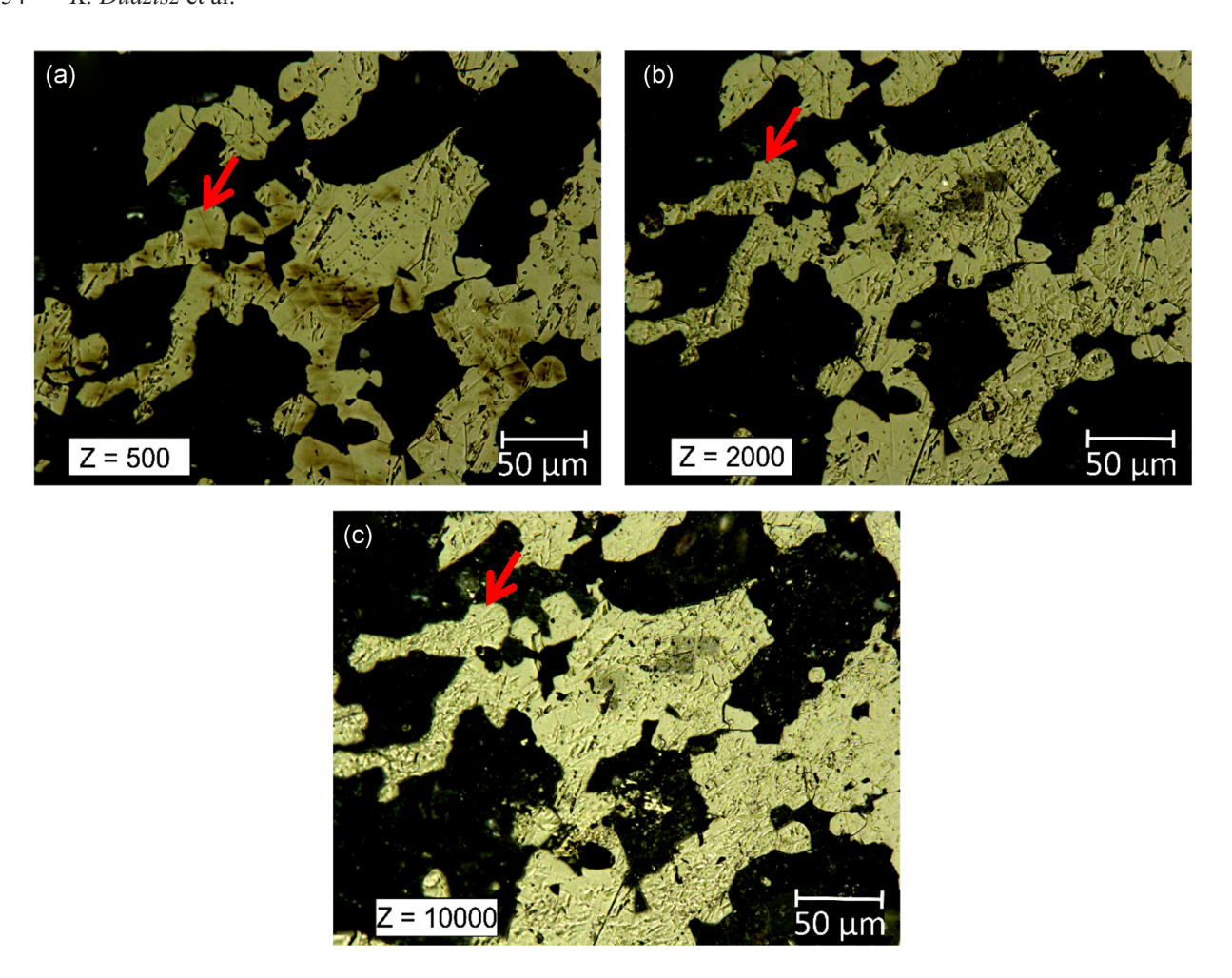


Figure 8. Reflected light micrographs of polished surface lying perpendicular to uniaxial compression of the cylindrical sample 28_{-1} compressed at 500° C in vacuum after (a) 500 cycles, (b) 2000 cycles and (c) $10\,000$ cycles. The red arrow marks a magnetite grain which surface roughness increases with the increasing cycle numbers (see details in the text).

cyclically loaded sample (Fig. 10a; see T_vP in Table 2) that might indicate some magnetic domain reduction in magnetite (Kontny et al. 2018). However, these changes are small as the Hopkinson peak ratio (HPR) from the heating and cooling curve indicates only a change from 1.12 to 1.28 in maximum (Table 2). Nevertheless, all treated samples show a small deviation in HPR between the heating and the cooling curves, which is not the case in the initial sample. Therefore, very small magnetic domain changes might occur and we have performed magnetic hysteresis measurements (Fig. 11a). The Day plot (Fig. 11b, Day et al. 1977) might indicate slight changes in the domain state of magnetite that are more or less in line with an increment of loading conditions. Only sample 500, which was only annealed, falls clearly in the PSD (pseudo-single domain, vortex) range. This behaviour might be explained by the formation of small haematite grains during heating and thus, shifting toward a higher ratio of M_r/M_s (Özdemir & Dunlop 2014). Fig. 12 shows the results of a combined analysis of surface (topography) and magnetic microstructure of an area containing boarded magnetite grains without (m1) and with fatigue stripes (m2). The topography features in this area revealed by AFM (Fig. 12a) are very similar to those observed by optical microscopy (Fig. 8). However, using a lift mode MFM relatively large domains (about 5 µm) are revealed within the upper grain (m1) exhibiting a relatively smooth surface (Fig. 12b). At the same time, the magnetic contrast inside the grain m2 suggests the presence of magnetic domains of submicrometre size (less than $0.1 \mu m$) inside of fatigue stripes.

4 DISCUSSION

4.1 The effect of various loading conditions on magnetic mineralogy and domain size

We studied the magnetic susceptibility and its anisotropy of a banded magnetite-quartz ore that was subjected to cyclic uniaxial loading (150 \pm 30 MPa) under elevated temperatures (400 and 500 $^{\circ} C)$ and compared it to samples that were only heated to test if the magnetic properties (magnetic susceptibility in particular) can be used to monitor early damage in magnetite. Our studies have shown that magnetic susceptibility decreases significantly within the first ca. 1000 cycles (Figs 3 and 7). The decrease is significantly stronger in air (up to 23 per cent) than in vacuum (up to 4 per cent) and stronger at 500 °C compared to 400 °C under both experimental conditions. As susceptibility also decreases for samples without cyclic loading, the main controlling factors for this decrease are temperature and time. Magnetic susceptibility was always measured after decompression of the loaded sample at room temperature (cycle steps, see Table 1, Supporting Information) or after a certain annealing time at 400 or 500 °C.

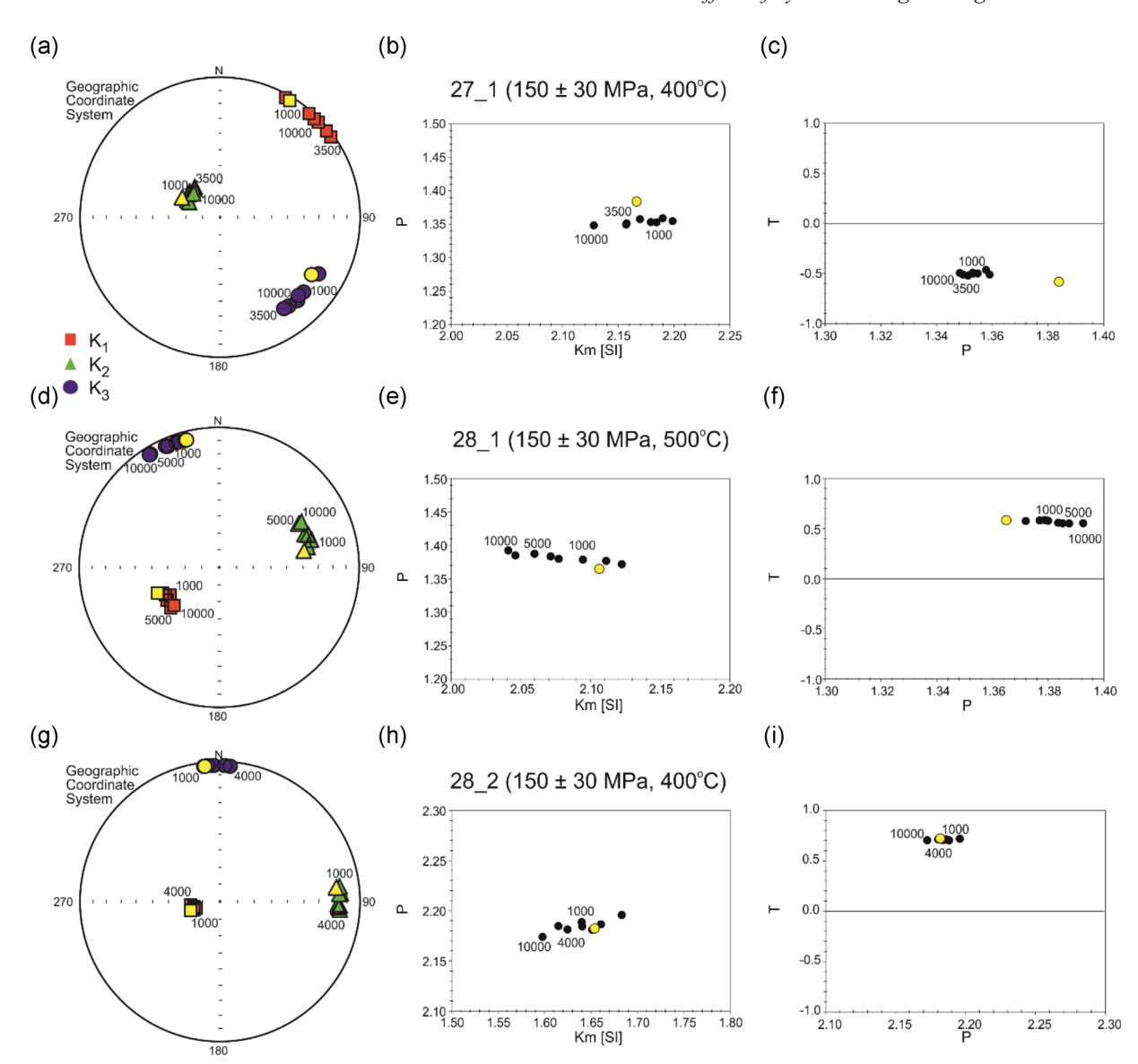


Figure 9. (a), (d), (g), (j), (m) and (p) Orientation of principal susceptibility axes after cyclic loading in vacuum and (b), (e), (h), (k), (n) and (q) changes in the degree of anisotropy (P) as a function of Km and (c), (f), (i), (l), (o) and (r) shape parameter. K_1 , K_2 and K_3 indicate maximum, intermediate and minimum susceptibility axes. Equal-area lower-hemisphere projections show results in the geographic coordinate system. Initial values and orientation of susceptibility axes are indicated in yellow.

Our study shows that initial loading conditions play an important role in the degree of alteration in rocks. Temperature and availability of oxygen are the most important factors controlling the rate of changes in the studied material (Figs 3 and 7). The higher the temperature at which samples were loaded the more pronounced is the oxidation of magnetite to haematite. The A_{40} index was proved to be a valuable tool for qualitative estimation of induced changes in magnetic mineralogy during laboratory experiments (e.g. Hrouda 2003; Just & Kontny 2012). In our study, we observed a trend in the A_{40} index from only annealed to static and cyclic deformed samples (Table 2). We interpret this observation to be related to stronger haematite formation in the deformed samples as new cracks develop, which increase oxidation. We have shown for the vacuum samples that intragranular microcrack formation is related to the number of cyclic loadings (Fig. 8), and suggest that the crack development favours the haematite formation in the air experiments. Chen et al. (2011) reported three stages of mechanical fatigue

starting from cracking on the boundaries (stage I) followed by intragranular deformation (stage II) and finally rocks' failure (stage III). Erarslan & William (2012) proved that grain boundaries are important for cracking initiation as stress concentrates at the grain boundaries and thus, enhances stronger oxidation into haematite in these areas as can be seen for our samples under the reflected light microscope (Fig. 4) and thus, the increasing values of A_{40} of air-treated samples are most likely the sum of effects caused by oxidation and deformation (Fig. 4).

In our studied magnetite grains (Fig. 8), the surface defects resemble persistent slip markings described in Polák & Man (2014, and references therein) for metals and metal alloys. Fatigue crack initiation is closely related to localization of cyclic strain in thin bands parallel to highly stressed crystallographic planes of the material (e.g. Cox & Clenshaw 1935; Forsyth 1953; Cottrell & Hull 1957; Karuskevich *et al.* 2012; Polák & Man 2014). These surface areas clearly show a distinct reduction of magnetic domain size

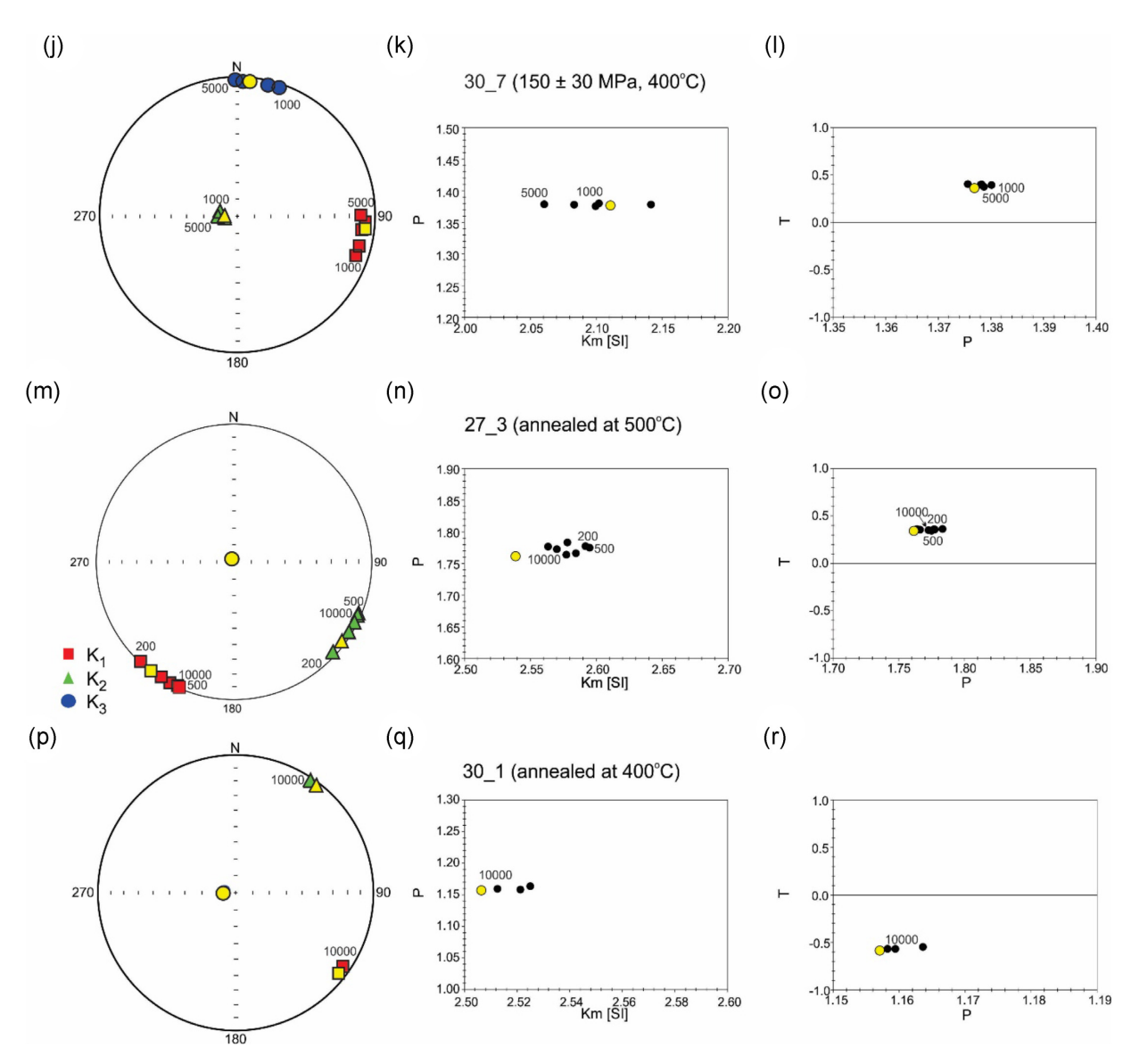


Figure 9. (Continued.)

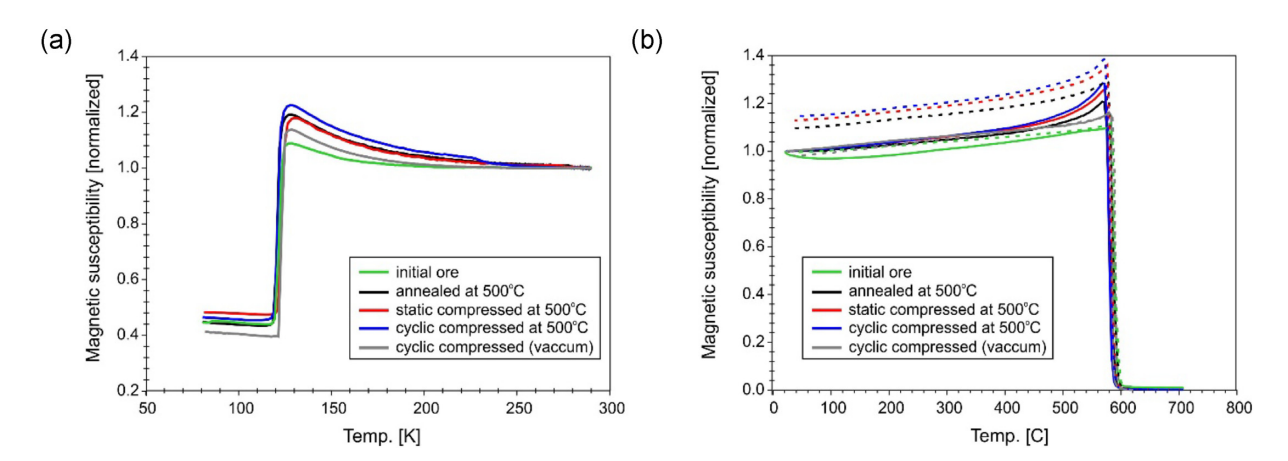


Figure 10. (a) Low- and (b) high-temperature magnetic susceptibility behaviour for samples subjected to different annealing and deformation conditions. In (b), the cooling curves are shown by dashed lines. The high-temperature measurements (b) were performed in an argon atmosphere. Curves were normalized to room temperature.

Table 2. Determination of the Verwey transition ($T_{\rm V}$), the Curie temperature on heating ($T_{\rm C}$ -h) and cooling ($T_{\rm c}$ -c) curves, $T_{\rm v}P$ (peak/room temperature ratio from the low-temperature curve), HPR-h, HPR-c (Hopkinson peak ratio from heating and cooling curve; see Dunlop 2014), and alteration index (A_{40}) for initial ore, sample annealed at 500 °C (500), static compressed samples at 500 °C (500CH) and cyclically loaded sample at 500 °C in vacuum (500CLV). The alteration index was calculated according to Hrouda *et al.* (2002). Hysteresis parameters: $M_{\rm s}$ —saturation magnetization, $M_{\rm r}$ —remanent magnetization, $B_{\rm c}$ —coercivity and $B_{\rm cr}$ —remanence coercivity.

Sample	Initial ore	500	500C	500CH	500CLV
$T_{ m V}$	118K	119K	121K	120K	121K
$T_{\rm C}$ -h	580 °C	577 °C	579 °C	578 °C	581 °C
$T_{\rm c}$ -c	584 °C	576 °C	586 °C	583 °C	587 °C
$T_{\rm v}P$	1.17	1.19	1.18	1.22	1.16
HPR-h	1.12	1.21	1.26	1.28	1.19
HPR-c	1.12	1.18	1.21	1.21	1.14
A_{40}	1.58	9.51	12.68	14.35	-2.28
M_{s}	66.57	34.74	36.81	42.84	67.56
$(Am^2 kg^{-1})$					
$M_{ m r}$	0.85	1.13	0.46	0.91	1.27
$(Am^2 kg^{-1})$					
$B_{\rm c}~({\rm mT})$	1.17	2.02	1.91	2.50	1.65
$B_{\rm cr}~({\rm mT})$	11.53	7.04	13.76	13.11	8.18

(~0.1 μm; see Fig. 12c), which confirm that stress concentration near grain boundaries and cracks occur. Magnetic domain patterns, especially at grain boundaries and near cracks, are often reported to be reduced due to stress and magnetoelastic anisotropy (e.g. Hubert & Schäfer 1998; Reznik *et al.* 2017).

There is no clear trend in bulk hysteresis data for the whole cylindrical volume of the samples in terms of reduction of domain size related to oxidation or cyclic loadings (Fig. 11). However, it can be observed that loading conditions change $B_{\rm cr}/B_{\rm c}$ ratio and move samples toward more PSD areas that might indicate a modification of the domain size and shape. As the studied material contain mainly multidomain (MD) grains, the decrease in susceptibility parallel to applied stress might be evidence for domain wall motion (Kean et al. 1976). The HPR (Table 2) indicate that magnetic domain sizes are not smaller than around an average of 10 μ m (Dunlop 2014), which is related to the formation of haematite that causes a reduction of magnetite's magnetic domains (Fig. 4) in the ambient airtreated samples. Even the systematically lower values of the HPR on cooling curves (Table 2) can be explained by the haematite as it retransforms during the temperature-dependent magnetic susceptibility measurement back to magnetite causing again an increase in magnetic domains. As annealing reduces internal stress and decreases microcoercivity in MD magnetite (Liu et al. 2008) this effect might also contribute to the lower HPR values (Kontny et al. 2018).

Nevertheless, the results of optical microscopy (Fig. 8) and MFM (Fig. 12) indicate that cyclic loading-induced microcracks and associated refinement of magnetic domains are critical indicators of mechanical fatigue in magnetite. According to Pokhil & Moskowitz (1997) as well as Williams *et al.* (1992), the magnetic contrast of the area inside m1 grain corresponds to well-defined Bloch walls in PSD or MD magnetite. In this case, dark contours can be interpreted as negative repulsion acts whilst positive ones as attraction acts. In the m2 grain containing persistent slip markings, the domain size is below 0.1 µm which indicates a single-domain (SD) range. We interpret the small magnetic susceptibility changes of a few per cent in the vacuum experiments to be related to the presence of SD

domains in the vicinity of persistent slip markings. It is worth mentioning that not all grains of magnetite are covered with persistent slip markings. The local strain accumulation strongly depends on the crystallographic orientation of magnetite single grains as well as stress redistribution defined by the local geometry of the surrounded quartz matrix. This interpretation needs further detailed studies, for example, by applying combined MFM and EBSD techniques (see e.g. in Batista *et al.* 2014).

4.2 The effect of various loading conditions on magnetic susceptibility and its anisotropy

Strong oxidation of magnetite to haematite during annealing only, annealing and loading in air causes a significant decrease in magnetic susceptibility and changes in P and T parameters (Fig. 3). Although only a small magnetic susceptibility decrease and no or only tiny changes in P and T parameters occur during vacuum experiments, we suggest that there is a small effect related to the uniaxial cyclic compression as a decrease in magnetic susceptibility is more pronounced for cyclically compressed samples at 500 °C compared to those that were only annealed at elevated temperatures (Figs 3a and b, and 7a and b). The degree of anisotropy increases linearly only in air-treated cyclic loaded samples at 500 °C but does not change visibly in all other samples. This change is accompanied by an increase in shape parameter T (Fig. 6). A reasonable explanation for the increase of P and possibly T values is a contribution of newly formed haematite that shows a strong single-crystal anisotropy that arises from a preferred orientation of platy crystals with P values > 100 (e.g. Flanders & Schuele 1964; Tarling & Hrouda 1993). Therefore, even a small degree of haematite alignment can cause significant changes in the degree of anisotropy.

It is also well known that the magnetic susceptibility of rocks decreases parallel to the applied stress axis and increases perpendicular to it (e.g. Nagata 1970). According to Kapička (1988), this behaviour causes a decrease in $P(K_1/K_3)$ and lineation factor (K_1/K_2) in magnetite. A stable orientation arrives when the K_3 axis is parallel to the direction of stress. However, after unloading the sample, the AMS ellipsoid reverts almost completely to its initial orientation (see fig. 5 in Kapička 1988). This reversibility is related to the piezomagnetic effect, which arises from the differential stress dependence of the magnetocrystalline anisotropy (Stacey 1964). In our experiments, the principal axes before and after the experiment were always closely clustered (Figs 6 and 9), but the vertical or steep directions (parallel to uniaxial load) always have better reversibility than the more horizontal axes (perpendicular to uniaxial load). Although this observation holds for all experimental conditions, we assume that the horizontal principal axis directions are stronger affected by the microcrack dilatancy which is related to haematite formation (Fig. 4) and persistent slip markings (Fig. 8) causing worse reversibility. Therefore, magnetostriction seems to play a minor role in the magnetic anisotropy behaviour of our cyclic loaded magnetite-quartz ore samples.

The development of cyclic compression-related deformation features occurs within a relatively small number of cycles (< 1000) after which the magnetic susceptibility reaches some saturation stage and no further decrease in magnetic susceptibility up to a maximum of 10 000 cycles is observed. The increase of crack-like defect density at the initial stages of compression (from 500 to 2000 cyclic loadings) is much more pronounced than for further loadings until 10 000 cycles in vacuum (Fig. 8), which suggests that the small magnetic susceptibility decrease in these samples is related to the

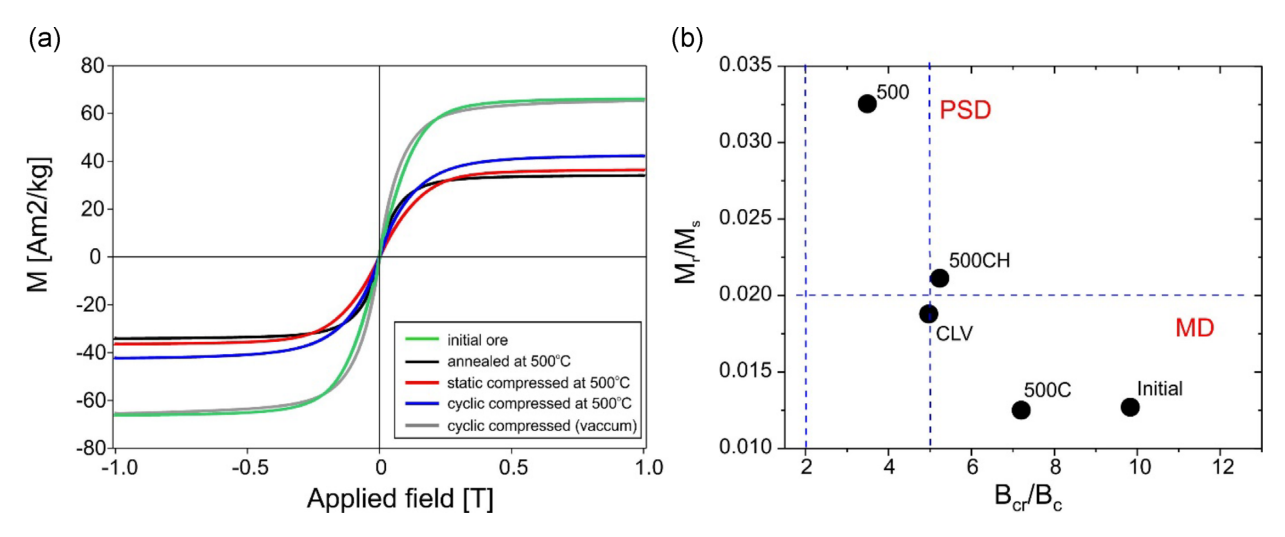


Figure 11. (a) Hysteresis curves and (b) Day plot (Day et al. 1977) for the initial and different treated magnetite ore samples subjected to various loading conditions. For sample description and experiment details, see Table 2.

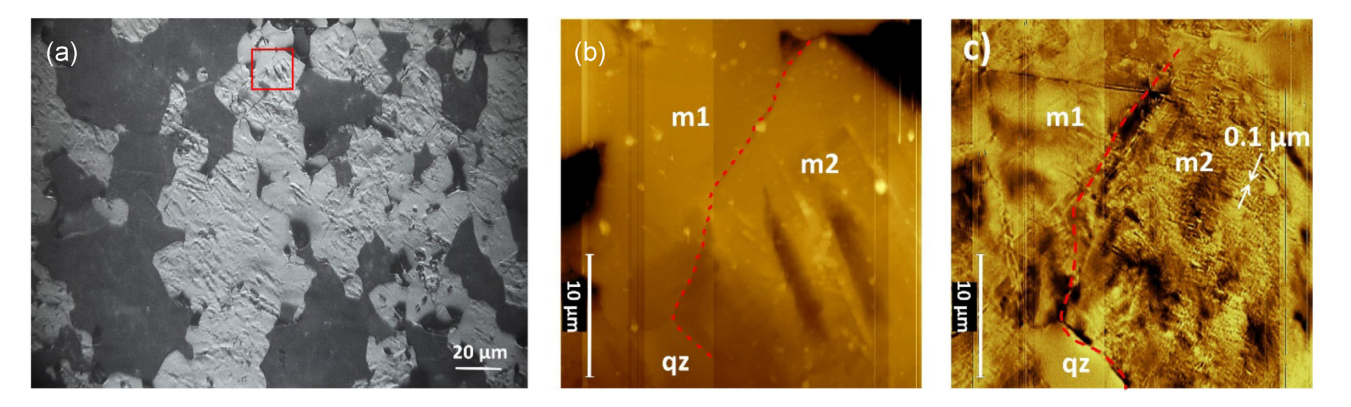


Figure 12. Direct observation of magnetic domain structures inside of the area shown by the red box in (a) for sample $28_{-}1$ (vacuum, $500\,^{\circ}$ C, 150 ± 30 MPa). (a) Reflected light image shows crack-like defects (called 'persistent slip markings' by Polák & Man 2014), (b) atomic force microscopy image showing the topography of two magnetite grains without (m1) and with persistent slip markings caused by fatigue deformation (m2). (c) MFM image taken from the same area shows a prominent refinement (\sim 0.1 μ m) of magnetic domains in grain m2 near the persistent slip markings. The red dashed line indicates the boundary between magnetite grains.

mechanical fatigue of magnetite. One explanation of the weakening effect under cyclic loading conditions is an increasing number of broken interparticle bonds producing a diffuse microfracture and decohesion of the rock after a predefined number of cycles (Cerfontaine & Collin 2018). This interpretation may also be applied to magnetite. The small decrease of magnetic susceptibility may indicate defects located at the surfaces of intragranular cracks and grain boundaries of the fatigued magnetite grains. Magnetic moments of surface atoms in magnetite decrease due to point defects at grain surfaces (Noh *et al.* 2015). The small increase in magnetic susceptibility, which was observed in some of the cyclically loaded samples in vacuum in the first cycling steps (Figs 7 a and b) might indicate some interaction of dislocation and point defects which can enhance the deformation resistance and cause cyclic hardening (Zhang *et al.* 2020).

Our results indicate that oxidation of magnetite to haematite, which is enhanced by the number of microcracks, are the dominant factors responsible for the decrease of magnetic susceptibility, and the change in AMS ellipsoid shape. Although ductile deformation is also known to increase the degree of anisotropy as there is a positive correlation between *P* and strain (Jackson *et al.* 1993; Till & Moskowitz 2013; Ferré *et al.* 2014), we do see only slight

plastic deformation in magnetite in our experiments. However, the transformation of magnetite into haematite and the microcracks in magnetite may change the shape of the grains.

5 CONCLUSIONS

The present study demonstrates the influence of temperature- and time-dependent cyclic loading conditions on magnetic susceptibility and its anisotropy of a magnetite-bearing ore. The first thousand cycles are the most sensitive for changes in magnetic susceptibility and its anisotropy. Further loadings do not significantly affect the magnetic susceptibility which then remains more or less constant. When oxygen is available during cyclic loading, mechanical fatigue in magnetite is accompanied by its partial transformation into haematite with a quite significant drop in magnetic susceptibility up to 23 per cent.

Vacuum experiments indicated only little changes in magnetic susceptibility up to 4 per cent as a result of irreversible deformation due to the formation of slip steps, whereas P and T do not show any trend or significant difference. This suggests that changes in the degree of anisotropy can be rather correlated with the formation of haematite from magnetite than to plastic deformation.

The increase of P and T values in air-treated samples can be either related to the change in the shape of the magnetite grains due to microcracks decorated by haematite or the effect of the strong single-crystal anisotropy of haematite. The intensity of oxidation is strongly dependent on temperature and time.

We have shown that even below 1000 cycles, cyclic loading can change significantly the induced magnetization of a rock due to mineral transformation and that the first stage of mechanical fatigue, which is a precursor of the failure of a rock, is closely associated with these transformations. However, it is questionable if time-dependent magnetic susceptibility measurements can be used in practice as an effective proxy parameter for the detection of mechanical fatigue because oxidation of magnetite to haematite can have manifold reasons in nature. Therefore, its application for the detection of seismomagnetic effects during geological engineering activities, especially in drilling operations or earthquake monitoring needs further studies.

ACKNOWLEDGEMENTS

This work was funded by Deutsche Forschungsgemeinschaft (DFG) Project 'Magnetic fatigue: effect of cyclic loading under elevated temperatures on the magnetic and structural behaviour' (KO1514/13–1 and WA2436/1–1). Many thanks to Martin Chadima from Agico for his support in understanding the differences in magnetic susceptibility in SUFAR and SUFAM mode. We thank the Institute for Rock Magnetism, Minneapolis for a visiting fellowship granted to BR in 2019 October and especially Mike Jackson for his support. We thank Stefan Walheim and Roland Gröger from the Karlsruhe Nano Micro Facility (KNMFi) at KIT for their friendly support during the MFM measurements and Tim Genssle for performing the MFM measurements. We wish to acknowledge the helpful comments of two anonymous reviewers.

DATA AVAILABILITY

All data for this study are included in the manuscript or Supporting Information.

REFERENCES

- Batista, L., Rabe, U. & Hirsekorn, S., 2014. Determination of the easy axes of small ferromagnetic precipitates in a bulk material by combined magnetic force microscopy and electron backscatter diffraction techniques, *Ultramicroscopy*, **146**, 17–26.
- Braunagel, M.J. & Griffith, W.A., 2019. The effect of dynamic stress cycling on the compressive strength of rocks, *Geophys. Res. Lett.*, 46, 6479–6486.
- Cerfontaine, B. & Collin, F., 2018. Cyclic and fatigue behaviour of rock materials: review, interpretation and research perspectives, *Rock Mech. Rock Eng.*, 51(2), 391–414.
- Chen, Y., Watanabe, K., Kusuda, H., Kusaka, E. & Mabuchi, M., 2011. Crack growth in Westerly granite during a cyclic loading test, *Eng. Geol.*, **117**(3-4), 189–197.
- Carporzen, L. & Gilder, S.A., 2010. Strain memory of the Verwey transition, J. geophys. Res. Solid Earth, 115, 1–12.
- Cottrell, A.H. & Hull, D., 1957. Extrusion and intrusion by cyclic slip in copper, Proc. R. Soc. A Math. Phys. Eng. Sci., 242, 211–213.
- Cox, H.L. & Clenshaw, W.J., 1935. The behaviour of three single crystals of aluminum in fatigue under complex stresses, *Proc. R. Soc. Lond. A.*, 149, 312–326.
- Day, R., Fuller, M. & Schmidt, V.A., 1977. Hysteresis properties of titanomagnetites: grain size and compositional dependence, *Phys. Earth planet. Inter.*, 13(4), 260–267.

- Dunlop, D.J., 2014. High-temperature susceptibility of magnetite: a new pseudo-single-domain effect, Geophys. J. Int., 199(2), 707–716.
- Ellwood, B.B., 1979. Sample shape and magnetic grain sizes: two possible controls on the anisotropy of magnetic susceptibility variability in deep-sea sediments, *Earth planet. Sci. Lett.*, **43**, 309–314.
- Erarslan, N. & Williams, D.J., 2012. Investigating the effect of cyclic loading on the indirect tensile strength of rocks, *Rock Mech. Rock Eng.*, 45, 327–340.
- Ferré, E.C., Gébelin, A., Till, J.L., Sassier, C. & Burmeister, K., 2014. Deformation and magnetic fabrics in ductile shear zones: a review, *Tectonophysics*, 629, 179–188.
- Flanders, P.J. & Schuele, W.J., 1964. Anisotropy in the basal plane of hematite single crystals, *Philos. Mag.*, 9(99), 485–490.
- Forsyth, P.J.E., 1953. Exudation of material from slip bands at the surface of fatigued crystals of an aluminum-copper alloy, *Nature*, **171**(4343), 172–173
- Gorkunov, E., Povolotskaya, A., Zadvorkin, S., Putilova, E. & Mushnikov, A., 2019. Effect of cyclic loading on the magnetic behaviour of hot-rolled pipe steel 08G2B, *Proc. Struct. Integr.*, 20, 4–8.
- Grosu, Y., Faik, A., Ortega-Fernández, I. & D'Aguanno, B., 2017. Natural magnetite for thermal energy storage: excellent thermophysical properties, reversible latent heat transition and controlled thermal conductivity, *Solar Energy Mater. Solar Cells*, 161, 170–176.
- Hao, J., Gu, Z. & Zhou, J., 1997. Anisotropy of magnetic susceptibility of rocks induced by experimental deformation, *Ann. Geophys.*, 40(2), 455–462.
- Hennig-Michaeli, C. & Siemes, H., 1982. Compression experiments on natural magnetite crystals at 200° C and 400° C at 400 MPa confining pressure, in *Issues in Rock Mechanics: Proceedings, Twenty-Third Symposium on Rock Mechanics, the University of California, Berkeley, California, August 25-27*(pp. 380), Berkeley, CA: American Rock Mechanics Association.
- Hrouda, F., 2003. Indices for numerical characterization of the alteration processes of magnetic minerals taking place during investigation of temperature variation of magnetic susceptibility, *Stud. Geophys. Geodaet.*, 47, 847–861.
- Hrouda, F, Chlupáčová, M. & Novák, J., 2002. Variations in magnetic anisotropy and opaque Mineralogy along a kilometer deep profile within a vertical dyke of the syenogranite porphyry at Cinovec (Czech Republic), J. Volc. Geotherm. Res., 113, 37–47.
- Hubert, A. & Schäfer, R., 1998. Magnetic Domains, the Analysis of Magnetic Microstructures, Springer-Verlag Berlin Heidelberg, 1998 ISBN: 978-3-540-64108-7 (Print).
- Jackson, M., Borradaile, G., Huddleston, P. & Banerjee, S., 1993. Experimental deformation of synthetic magnetite-bearing calcite sandstones: effects on remanence, bulk magnetic properties, and magnetic anisotropy, *J. geophys. Res.*, 98, 383–401.
- Jelínek, V., 1981. Characterization of the magnetic fabric of rocks, *Tectono-physics*, 79, 63–67.
- Johnston, A.C., 1989. The Effect of Large Ice Sheets on Earthquake Genesis, In: Earthquakes at North-Atlantic Passive Margins: Neotectonics and Postglacial Rebound. NATO ASI Series (Series C: Mathematical and Physical Sciences), vol 266. Springer, Dordrecht.
- Johnston, M.J.S., Sasai, Y., Egbert, G.D. & Mueller, R.J., 2006. Seismomagnetic effects from the long-awaited 28 September 2004 M 6.0 Parkfield earthquake, *Bull. seism. Soc. Am.*, 96(4B), S206–S220.
- Johnson, P.A. & Jia, X., 2005. Nonlinear dynamics, granular media and dynamic earthquake triggering, *Nature*, 437, 871–874.
- Just, J. & Kontny, A., 2012. Thermally induced alterations of minerals during measurements of the temperature dependence of magnetic susceptibility: a case study from the hydrothermally altered Soultz sous-Forêts granite, France, *Int. J. Earth Sci.*, **101**, 819–839.
- Kalkhof, D., Grosse, M., Niffenegger, M. & Leber, H.J., 2004. Monitoring fatigue degradation in austenitic stainless steels, *Fatigue Fract. Eng. Mater. Struct.*, 27, 595–607.
- Kapička, A., 1988. Anisotropy of magnetic susceptibility in a weak magnetic field induced by stress, *Phys. Earth planet. Inter.*, 51(4), 349–354.

- Karuskevich, M., Karuskevich, O., Maslak, T. & Schepak, S., 2012. Extrusion/intrusion structures as quantitative indicators of accumulated fatigue damage, *Int. J. Fatigue*, 39, 116–121.
- Kean, W.F., Day, R., Fuller, M. & Schmidt, V.A. 1976. The effect of uniaxial compression on the initial susceptibility of rocks as a function of grain size and composition of their constituent titanomagnetites, *J. geophys. Res.*, 81, 861–872.
- Kontny, A., Reznik, B., Boubnov, A., Göttlicher, J. & Steininger, R., 2018. Post-shock thermally induced transformations in experimentally shocked magnetite, *Geochem. Geophys, Geosys.*, 19, 921–931.
- Leng, J., Xu, M., Xu, M. & Zhang, J., 2009. Magnetic field variation induced by cyclic bending stress, NDT E Int., 42(5), 410–414.
- Liang, W., Zhang, C., Gao, H., Yang, X., Xu, S. & Zhao, Y., 2012. Experiments on mechanical properties of salt rocks under cyclic loading, J. Rock Mech. Geotech. Eng., 4(1), 54–61.
- Lin, A., 2008. Seismic slip in the lower crust inferred from granulite-related pseudotachylyte in the Woodroffe Thrust, central Australia, *Pure appl. Geophys.*, 165, 215–233.
- Liu, Q., Yu, Y., Muxworthy, A.R. & Roberts, A.P., 2008. Effects of internal stress on remanence intensity jumps across the Verwey transition for multi-domain magnetite, *Phys. Earth planet. Inter.*, 169(1–4), 100–107.
- Martin, R.J., Habermann, R.E. & Wyss, M., 1978. The effect of stress cycling and inelastic volumetric strain on remanent magnetization, *J. geophys. Res.*, 83(B7), 3485–3496.
- Nagata, T., 1961. Rock Magnetism, Maruzen Company LTD., Tokyo.
- Nagata, T., 1970. Basic magnetic properties of rocks under the effects of mechanical stresses, *Tectonophysics*, 9(2-3), 167–195.
- Nagata, T. & Kinoshita, H., 1964. Effect of release of compression on magnetization of rocks and assemblies of magnetic minerals, *Nature*, 204, 1183–1184.
- Noh, J., Osman, O.I., Aziz, S.G., Winget, P. & Brédas, J.L., 2015. Magnetite Fe3O4 (111) surfaces: impact of defects on structure, stability, and electronic properties, *Chem. Mater.*, 27(17), 5856–5867.
- Owens, W.H., 1974. Mathematical model studies on factors affecting the magnetic anisotropy of deformed rocks, *Tectonophysics*, 24, 115–131.
- Özdemir, Ö. & Dunlop, D.J., 2014. Hysteresis and coercivity of hematite, J. geophys. Res. Solid Earth, 119, 2582–2594.
- Pokhil, T.G. & Moskowitz, B. M. 1997. Magnetic domains and domain walls in pseudo-single domain magnetite studied with magnetic force microscopy, *J. geophys. Res.*, 102(B10), 22681–22694.
- Polák, J. & Man, J., 2014. Mechanisms of extrusion and intrusion formation in fatigued crystalline materials, *Mater. Sci. Eng. A*, 596, 15–24.
- Rao, M.V.M.S. & Ramana, Y.V., 1992. A study of progressive failure of rock under cyclic loading by ultrasonic and AE monitoring techniques, *Rock Mech. Rock Eng.*, 25, 237–251.

- Reznik, B., Kontny, A., Fritz, J. & Gerhards, U., 2016. Shock-induced deformation phenomena in magnetite and their consequences on magnetic properties, *Geochem., Geophys. Geosys.*, 17, 2374–2393.
- Reznik, B., Kontny, A., Uehara, M., Gattacceca, J., Solheid, P. & Jackson, M., 2017. Magnetic domains and magnetic stability of cohenite from the Morasko iron meteorite, *J. Magn. Magn. Mater.*, 426, 594–609.
- Stacey, F.D., 1961. Theory of the magnetic properties of igneous rocks in alternating fields, *Philos. Mag.*, **6**, 1241–1260.
- Stacey, F.D., 1964. The Seismomagnetic Effect, *Pure appl. Geophys.*, **58**(II), 5–22.
- Stacey, F.D. & Johnston, M.J.S., 1972. Theory of the piezomagnetic effect in titanomagnetite bearing Rocks, *Pure appl. Geophys.*, 97(1), 146–155.
- Stacey, F.D. & Westcott, P., 1965. Seismomagnetic effect- limit of observability imposed by local variations in geomagnetic disturbances, *Nature*, 206(4990), 1209–1211.
- Stoner, E.C., 1945. XCVII. The demagnetizing factors for ellipsoids, The London, Edinburgh, and Dublin, *Philos. Mag. J. Sci.*, 36(263), 803–821.
- Tarling, D.H. & Hrouda, F., 1993. The Magnetic Anisotropy of Rocks, Chapman and Hall, London, UK.
- Till, J.L. & Moskowitz, B., 2013. Magnetite deformation mechanism maps for better prediction of strain partitioning, *Geophys. Res. Lett.*, 40, 697– 702.
- Till, J.L., Moskowitz, B.M. & Jackson, M.J., 2012. High-temperature magnetic fabric development from plastically deformed magnetite in experimental shear zones, *Geophys. J. Int.*, 189, 229–239.
- Till, J.L., Rybacki, E., Morales, L.F.G. & Naumann, M., 2019. High-temperature deformation behaviour of synthetic polycrystalline magnetite, J. geophys. Res.: Solid Earth, 124, 2378–2394.
- Uyeda, S., Fuller, M.D., Belshé, J.C. & Girdler, R.W., 1963. Anisotropy of magnetic susceptibility of rocks and minerals, *J. geophys. Res.*, 68, 279–291.
- Violay, M., Heap, M.J., Acosta, M. & Madonna, C., 2017. Porosity evolution at the brittle-ductile transition in the continental crust: implications for deep hydro-geothermal circulation, Sci. Rep., 7, 7705.
- Volk, M.W.R. & Feinberg, J.M., 2019. Domain state and temperature dependence of pressure remanent magnetization in synthetic magnetite: implications for crustal remagnetization, *Geochem., Geophys. Geosys.*, 20, 2473–2483.
- Williams, W., Hoffmann, V., Heider, F., Göddenhenrich, T. & Heiden, C., 1992. Magnetic force microscopy imaging of domain walls in magnetite, Geophys. J. Int., 111(3), 417–423.
- Zhang, K., Walter, M. & Aktaa, J., 2020. Ratcheting and fatigue behaviour of Eurofer97 at high temperature, part1: experiment, *Fusion Eng. Des.*, **150**, 111407.